

# Overexpression of Arabidopsis ACBP3 Enhances NPR1-Dependent Plant Resistance to *Pseudomonas syringae* pv *tomato* DC3000<sup>1[W][OA]</sup>

Shi Xiao and Mee-Len Chye\*

School of Biological Sciences, The University of Hong Kong, Pokfulam, Hong Kong, China

*ACBP3* is one of six Arabidopsis (*Arabidopsis thaliana*) genes, designated *ACBP1* to *ACBP6*, that encode acyl-coenzyme A (CoA)-binding proteins (ACBPs). These ACBPs bind long-chain acyl-CoA esters and phospholipids and are involved in diverse cellular functions, including acyl-CoA homeostasis, development, and stress tolerance. Recombinant ACBP3 binds polyunsaturated acyl-CoA esters and phospholipids in vitro. Here, we show that ACBP3 plays a role in the plant defense response to the bacterial pathogen *Pseudomonas syringae* pv *tomato* DC3000. *ACBP3* mRNA was up-regulated upon pathogen infection and treatments using pathogen elicitors and defense-related phytohormones. Transgenic Arabidopsis *ACBP3* overexpressors (*ACBP3-OEs*) showed constitutive expression of pathogenesis-related genes (*PR1*, *PR2*, and *PR5*), cell death, and hydrogen peroxide accumulation in leaves. Consequently, *ACBP3-OEs* displayed enhanced resistance to the bacterial pathogen *P. syringae* DC3000. In contrast, the *acbp3* T-DNA insertional mutant was more susceptible and exhibited lower *PR* gene transcript levels upon infection. Using the *ACBP3 OE-1* line in combination with *nonexpressor of PR genes1 (npr1-5)* or *coronatine-insensitive1 (coi1-2)*, we concluded that the enhanced *PR* gene expression and *P. syringae* DC3000 resistance in the *ACBP3-OEs* are dependent on the NPR1-mediated, but not the COI1-mediated, signaling pathway. Given that *ACBP3-OEs* showed greater susceptibility to infection by the necrotrophic fungus *Botrytis cinerea* while the *acbp3* mutant was less susceptible, we suggest that ACBP3 plays a role in the plant defense response against biotrophic pathogens that is distinct from necrotrophic pathogens. ACBP3 function in plant defense was supported further by bioinformatics data showing up-regulation of many biotic and abiotic stress-related genes in *ACBP3 OE-1* in comparison with the wild type.

The acyl-CoA-binding proteins (ACBPs) are conserved at the ACB domain (Xiao and Chye, 2009, 2011). They have been identified from various organisms, including plants, yeast, *Drosophila*, and mammals, and implicated in diverse functions such as acyl-CoA and/or phospholipid metabolism, acyl-CoA trafficking and homeostasis, protection of acyl lipids from cytosolic enzymes, growth, development, and stress tolerance (Knudsen et al., 2000; Faergeman and Knudsen, 2002; Xiao and Chye, 2009, 2011; Yurchenko et al., 2009; Fan et al., 2010; Yurchenko and Weselake, 2011). In addition to the 10-kD ACBPs, which are ubiquitous in eukaryotes, larger forms of ACBPs have been identified from many species (Leung et al., 2004; Xiao and Chye, 2009; Fan et al., 2010; Meng et al., 2011). For example, in the model plant Arabidopsis (*Arabidopsis*

*thaliana*), in a total of six ACBPs (*ACBP1*–*ACBP6*), five are larger than 10 kD (Engeseth et al., 1996; Chye, 1998; Chye et al., 2000; Leung et al., 2004; Chen et al., 2008; Xiao and Chye, 2009), while in rice (*Oryza sativa*), four of six ACBPs exceed 10 kD (Meng et al., 2011). Functional analyses of the Arabidopsis ACBPs have revealed that despite conservation in the ACB domain, they vary in size from 92 amino acids (10.4 kD) to 668 amino acids (73.1 kD), are located in different cellular compartments, and show distinct in vitro binding affinities to acyl-CoA/phospholipid substrates, suggesting that they may play nonredundant functions in planta (Xiao and Chye, 2009, 2011; Yurchenko and Weselake, 2011). Arabidopsis ACBPs have been demonstrated to serve various roles in lipid metabolism, in early embryo development (Chen et al., 2010) and senescence (Xiao et al., 2010), as well as in conferring tolerance to heavy metals (Xiao et al., 2008a; Gao et al., 2009, 2010) and freezing (Chen et al., 2008; Du et al., 2010).

Among the Arabidopsis ACBPs, three members (*ACBP1*, *ACBP2*, and *ACBP3*) contain N-terminal transmembrane domains and are membrane associated, with *ACBP3* also being targeted to the apoplast (Chye, 1998; Chye et al., 1999, 2000; Li and Chye, 2003, 2004; Leung et al., 2006; Xiao et al., 2010). *ACBP3* is unique in its domain structure in comparison with other large Arabidopsis ACBPs because it lacks ankyrin repeats or kelch motifs, and it is the only large ACBP

<sup>1</sup> This work was supported by the Research Grants Council of the Hong Kong Special Administrative Region, China (project no. HKU7047/07M), and the University of Hong Kong (project no. 10208034 and postdoctoral fellowship to S.X.).

\* Corresponding author; e-mail mlchye@hkucc.hku.hk.

The author responsible for distribution of materials integral to the findings presented in this article in accordance with the policy described in the Instructions for Authors (www.plantphysiol.org) is: Mee-Len Chye (mlchye@hkucc.hku.hk).

<sup>[W]</sup> The online version of this article contains Web-only data.

<sup>[OA]</sup> Open Access articles can be viewed online without a subscription.

www.plantphysiol.org/cgi/doi/10.1104/pp.111.176933

identified so far that has an ACB domain located at the C terminus (Leung et al., 2004; Xiao and Chye, 2011). Previous studies have revealed that its ACB domain binds to C18- and C20:4-acyl-CoA esters as well as C18- phosphatidylethanolamine (PE) in vitro (Leung et al., 2006; Xiao et al., 2010). Our investigations show correlation between *ACBP3* expression and PE composition in vivo; for example, PE levels increase in *Arabidopsis ACBP3* overexpressors (*ACBP3-OEs*) and decrease in *ACBP3* knockout lines (*ACBP3-KOs*) comprising the *acbp3* T-DNA insertional mutant and RNA interference lines (Xiao et al., 2010). Furthermore, the *ACBP3-OE* and *ACBP3-KO* lines exhibited accelerated and delayed leaf senescence phenotypes, respectively. Our observations of disrupted autophagosome formation accompanied by an enhanced degradation of the GFP-ATG8e protein, a translational fusion of GFP to the autophagy protein 8e (ATG8e), in the combined *ACBP3 OE-1 GFP-ATG8e* line during starvation have linked *ACBP3* function to the regulation of ATG8-PE complex formation and autophagy-mediated leaf senescence (Xiao et al., 2010). The autophagy pathway is a highly regulated process essential for bulk degradation and nutrient recycling in many species (Ohsumi, 2001; Levine and Klionsky, 2004). In plants, the autophagy proteins (ATGs) have been reported to be related to salicylic acid (SA) signaling-dependent plant innate immunity-associated programmed cell death (PCD; Liu et al., 2005; Yoshimoto et al., 2009). Hence, it was pertinent to investigate the potential role of *ACBP3* in this process, given its abilities to interact with PE and to modulate ATG8 stability.

Here, *ACBP3* mRNA expression was observed to be induced following bacterial pathogen infection as well as pathogen elicitor and defense-related phytohormone treatments. Consequently, alterations in *ACBP3* expression in *ACBP3-OE* and *acbp3* mutant lines were found to affect responses to bacterial pathogen infection, suggesting a role for *ACBP3* in plant defense that was investigated further using SA signaling (*nonexpressor of PR genes1* [*npr1-1* and *npr1-5*]) and jasmonic acid (JA) signaling (*coronatine-insensitive1* [*coi1-2*]) mutants.

## RESULTS

### *ACBP3* Expression Is Induced by Phytopathogens, Arachidonic Acid, and Phytohormones

To examine the potential role of *ACBP3* in plant defense, *ACBP3* mRNA expression following fungal or bacterial pathogen infection was analyzed in RNA gel-blot analyses. As shown in Figure 1A, the expression of *ACBP3* is induced 12, 24, and 48 h post inoculation (hpi) with either *Botrytis cinerea* or *Pseudomonas syringae* pv *tomato* DC3000. *ACBP3* expression was also elevated following treatment with the fungal elicitor arachidonic acid (AA; Fig. 1B).

As the phytohormones ethylene, JA, and SA are known to regulate plant defense response, *ACBP3*

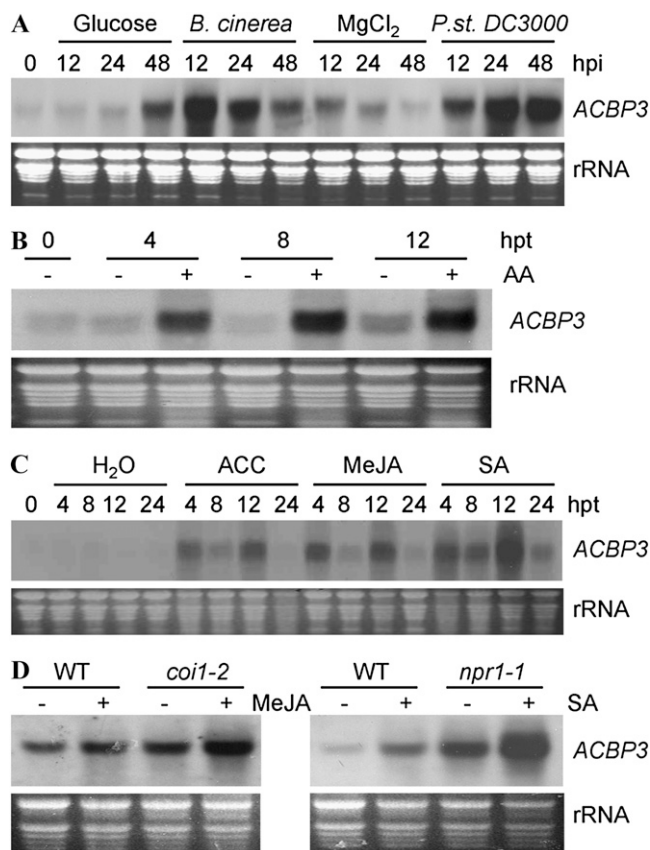


**Figure 1.** RNA gel-blot analyses using a DIG-labeled *ACBP3* cDNA probe to investigate the expression patterns of *ACBP3*. A, *ACBP3* expression is induced by phytopathogens. Total RNA samples from 3-week-old soil-grown wild-type *Arabidopsis* seedlings were infected with *B. cinerea* or *P. syringae* DC3000 with 1% Glc and 10 mM  $MgCl_2$  as mock controls, respectively, and harvested at 0, 12, 24, and 48 hpi for RNA gel-blot analysis. B, *ACBP3* expression is induced by AA. Total RNA samples from 3-week-old wild-type *Arabidopsis* seedlings grown on MS medium were treated with water (–) or AA (+) and harvested at 0, 4, 8, and 12 h post treatment (hpt) for RNA gel-blot analysis. C, *ACBP3* expression is induced in response to ACC, MeJA, and SA treatments. Total RNA samples from 3-week-old wild-type *Arabidopsis* seedlings grown on MS medium were treated with water, 1 mM ACC, 100  $\mu$ M MeJA, or 1 mM SA and harvested at 0, 4, 8, 12, and 24 h post treatment for RNA gel-blot analysis. D, The expression of *ACBP3* in the wild type (WT), *coi1-2*, and *npr1-1*. Total RNA samples from 3-week-old wild-type, *coi1-2*, and *npr1-1* plants treated with water (–) and 100  $\mu$ M MeJA (+) or 1 mM SA (+) were collected at 8 h post treatment for RNA gel-blot analysis. Ethidium bromide-stained rRNAs are shown below the blots to indicate the relative amounts of total RNA loaded per lane. Blots were repeated with similar results.

expression in response to 1-aminocyclopropane-1-carboxylic acid (ACC; the direct precursor of ethylene), methyl jasmonate (MeJA), and SA was determined. Results from RNA gel-blot analysis revealed that *ACBP3* mRNA was induced after treatment with 1 mM ACC, 100  $\mu$ M MeJA, or 1 mM SA at 4, 8, 12, and 24 h post treatment (Fig. 1C). These findings indicate that *ACBP3* expression is up-regulated upon pathogen infection and treatment with the phytohormones ACC, MeJA, and

SA, suggesting that ACBP3 function may be associated with plant defense. It has been noted that the up-regulation of *ACBP3* changes at different time points upon ACC, MeJA, or SA treatment, and this may have been caused by variation in light conditions, because the *ACBP3* transcript is regulated by light/dark cycling (Xiao et al., 2009, 2010).

To explore further the relationship between ACBP3 and the JA and/or SA signaling pathways, its expression in the JA signaling-deficient *coi1-2* mutant (Xiao et al., 2004) and the SA signaling-deficient *npr1-1* mutant (Cao et al., 1994) was examined. Results from RNA gel-blot analyses showed an up-regulation of *ACBP3* mRNA in both *coi1-2* and *npr1-1* (Fig. 1D) mutants in comparison with the wild type, with a marked increase in *npr1-1* after SA treatment (Fig. 1D). The slightly JA-inducible expression of *ACBP3* in the *coi1-2* mutant may be because the *coi1-2* mutation is a leaky allele in JA-responsive gene expression as well as in male fertility (Xiao et al., 2004).

#### Overexpression of *ACBP3* Constitutively Activates *PR* Gene Expression and Promotes Cell Death and Hydrogen Peroxide Production

The expression levels of pathogenesis-related genes (*PR1*, *PR2*, *PR5*, and *PDF1.2*) in the *ACBP3-OE* lines (Xiao et al., 2010) were investigated further by RNA gel-blot analysis using PCR-generated digoxigenin (DIG)-labeled *PR1*, *PR2*, *PR5*, and *PDF1.2* probes. As shown in Figure 2A, *PR1*, *PR2*, and *PR5* mRNAs were constitutively activated in all three independent *ACBP3-OE* lines tested (*OE-1*, *OE-4*, and *OE-6*), while the expression of *PDF1.2* was down-regulated. Subsequently, the *OE-1* and *OE-4* lines were used for further analysis, since they have been phenotypically and biochemically characterized previously (Xiao et al., 2010).

Plants showing SA-dependent constitutive disease resistance are characterized by the occurrence of spontaneous lesions and the generation of high levels of reactive oxygen species (Xia et al., 2004; Glazebrook, 2005). To examine whether *ACBP3-OE*s show cell death and reactive oxygen species accumulation, the rosettes of *OE-1* and *OE-4* lines were tested using trypan blue and diaminobenzidine (DAB) staining analyses. Lesions were apparent upon trypan blue staining in the leaves of uninfected *ACBP3-OE* plants (*OE-1* and *OE-4*) but not in the wild type (Fig. 2B). When DAB staining was used to detect hydrogen peroxide ( $H_2O_2$ ) in situ, the uninfected leaves of *ACBP3-OE* appeared to have generated high levels of  $H_2O_2$ , as detected by a yellow color, in contrast to the uninfected wild type (Fig. 2C).

#### *ACBP3-OE*s Show Enhanced Protection against a Bacterial Pathogen

Given that *ACBP3* expression appeared to be associated with the plant defense response (Fig. 1A), an investigation was conducted to examine whether a change in *ACBP3* expression would affect plant disease susceptibility. Wild-type and *ACBP3-OE* (*OE-1* and *OE-4*) seedlings were inoculated with the virulent strain of the bacterial pathogen *P. syringae* pv *tomato* DC3000 (Fig. 3A). Four days after inoculation (dai), the leaves of wild-type plants showed severe chlorosis in response to infection (Fig. 3A), while the leaves of *OE-1* and *OE-4* lines displayed little yellowing (Fig. 3A), suggesting that the *ACBP3-OE* plants were conferred resistance to this pathogen. When the inoculated plants were analyzed further, it was revealed that bacterial growth, as measured by counting bacterial numbers at 4 dai in the *ACBP3-OE* lines, were about 3-fold lower than in the wild type (Fig. 3B), confirming

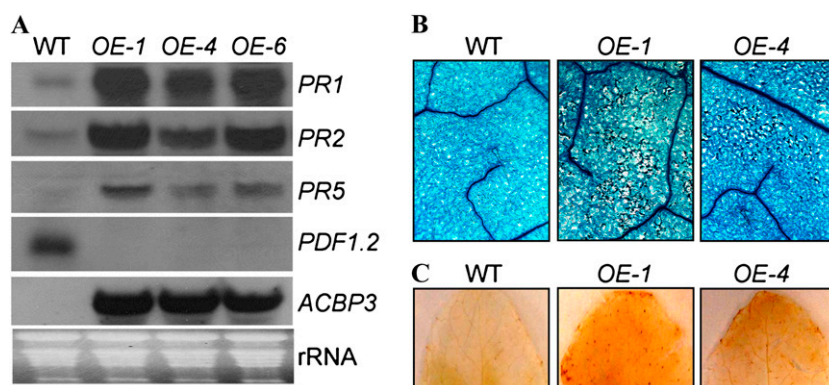


**Figure 2.** Overexpression of *ACBP3* mRNA causes constitutive expression of the pathogenesis-related genes (*PR1*, *PR2*, and *PR5*) and promotes cell death and  $H_2O_2$  production. A, RNA gel-blot analysis showing expression of *ACBP3*, *PR1*, *PR2*, *PR5*, and plant defensin *PDF1.2* in wild-type (WT) and *ACBP3-OE* (*OE-1*, *OE-4*, and *OE-6*) plants. Total RNA samples extracted from 10-d-old seedlings germinated and grown on MS medium were loaded (30  $\mu$ g per well) for gel electrophoresis, blotted, and hybridized to DIG-labeled cDNA probes of *ACBP3* (1.3 kb), *PR1* (0.45 kb), *PR2* (1.0 kb), *PR5* (0.6 kb), and *PDF1.2* (0.45 kb), where transcript lengths are given in parentheses. At bottom is an ethidium bromide-stained gel before blotting showing rRNA bands. Blots were repeated with similar results. B, Trypan blue staining shows small clusters of dead cells in the uninfected *ACBP3-OE* leaves but not in the wild type. C, DAB staining shows localized  $H_2O_2$  production in uninfected *ACBP3-OE* leaves but not in the wild type.

that an overexpression of Arabidopsis *ACBP3* had culminated in an enhanced resistance to *P. syringae* infection.

The responses of the *ACBP3*-KOs, including the *acbp3* T-DNA insertional mutant and the *ACBP3* RNA interference (RNAi) transgenic line *RNAi-1* (Xiao et al., 2010), to bacterial pathogen inoculation were tested next and compared with wild-type and *OE* lines. As shown in Figure 4A, the bacterium-infected *acbp3* mutant and *RNAi-1* plants displayed higher bacterial counts than the wild type at 4 dai (Fig. 4A). The 2.6- and 2.7-fold increases in bacterial count in the *acbp3* mutant and *RNAi-1* plants, respectively, were deemed significant ( $P < 0.05$  by Student's *t* test; Fig. 4A). To investigate whether the expression of plant defense genes *PR1*, *PR2*, and *PR5* were affected in the *acbp3*

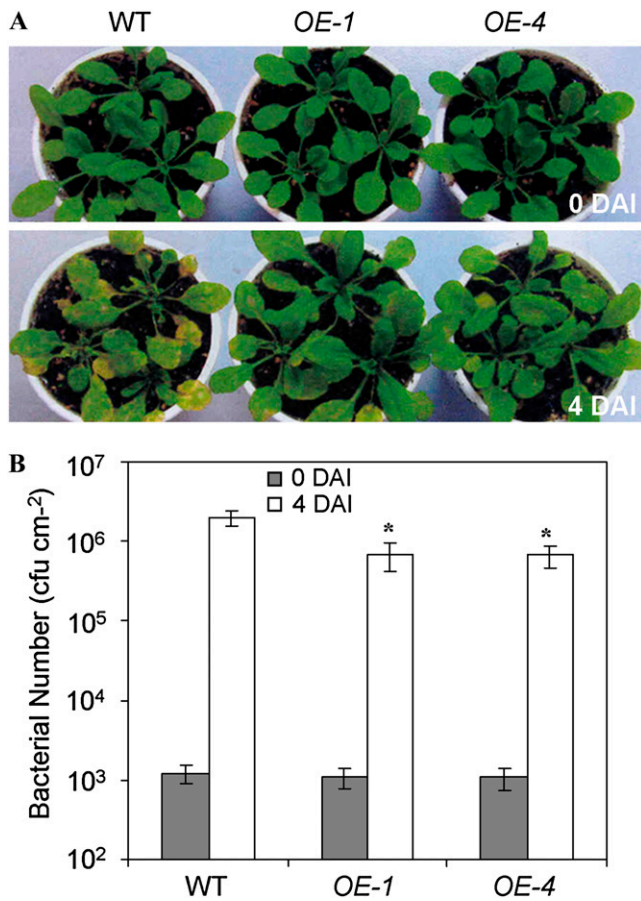


**Figure 3.** *ACBP3*-OEs show enhanced resistance to *P. syringae* DC3000 infection. A, Three-week-old wild-type (WT) and *ACBP3*-OE (*OE-1* and *OE-4*) plants were inoculated with *P. syringae* DC3000. Plants were sprayed with bacterial suspension ( $OD_{600} = 0.01$ ) and photographed at 0 and 4 dai. The yellowing in the wild-type leaves at 4 dai indicates infection. The experiment was repeated with similar results. B, Bacterial growth in wild-type, *OE-1*, and *OE-4* plants at 0 and 4 dai. Data points represent means of three replicates (each replicate was pooled with three leaf discs) taken from three independent plants, and bacterial counts were determined on a per cm<sup>2</sup> basis. cfu, Colony-forming units. \*  $P < 0.05$  by Student's *t* test.

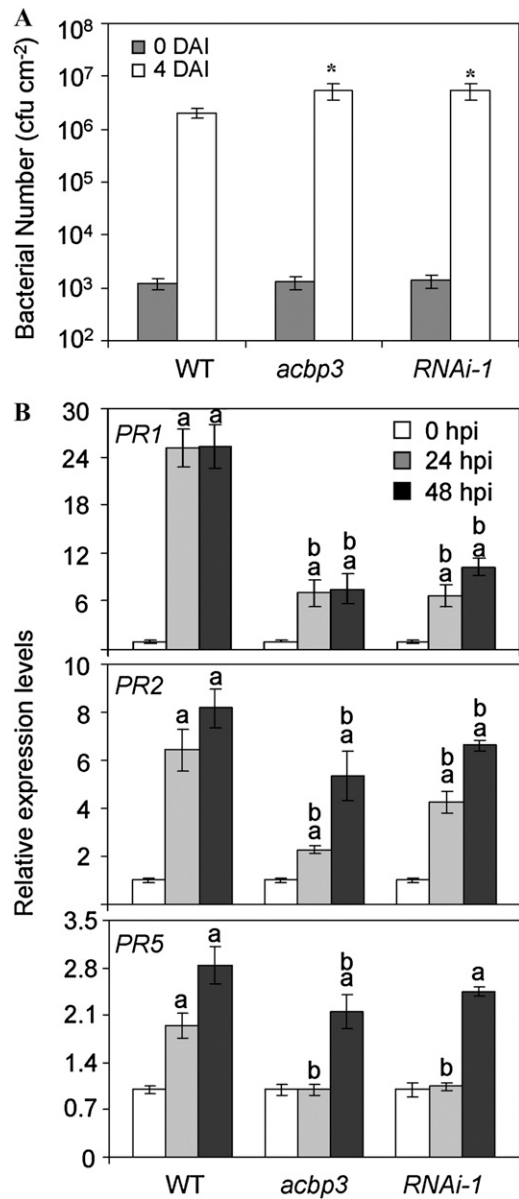


**Figure 4.** The *ACBP3*-KOs show increased susceptibility to *P. syringae* DC3000 infection. A, Bacterial growth in wild-type (WT), *acbp3* mutant, and *ACBP3 RNAi-1* plants at 0 and 4 dai. Data points represent means of three replicates (each replicate was pooled with three leaf discs) taken from three independent plants, and bacterial counts were determined on a per cm<sup>2</sup> basis. The experiment was repeated with similar results. \*  $P < 0.05$  by Student's *t* test. B, qRT-PCR analyses showing the expression of *PR1*, *PR2*, and *PR5* in wild-type, *acbp3* mutant, and *ACBP3 RNAi-1* plants before and after infection. Rosettes of 3-week-old wild-type, *acbp3* mutant, and *ACBP3 RNAi-1* plants were syringe infiltrated with bacterial suspension ( $OD_{600} = 0.001$ ) and harvested at 0, 24, and 48 hpi. Expression levels for each gene in the wild type, *acbp3* mutant, and *ACBP3 RNAi-1* at 0, 24, and 48 hpi were normalized to uninfected (0-hpi) wild-type, *acbp3* mutant, and *ACBP3 RNAi-1* values, respectively. cfu, Colony-forming units. Letters above bars are as follows: <sup>a</sup> significant difference ( $P < 0.05$  by Student's *t* test) in the wild type, *acbp3* mutant, or *ACBP3 RNAi-1* at 24 and 48 hpi when compared with 0-hpi wild-type, *acbp3* mutant, or *ACBP3 RNAi-1* plants; <sup>b</sup> significant difference ( $P < 0.05$  by Student's *t* test) between the wild type, *acbp3* mutant, or *ACBP3 RNAi-1* at 24 and 48 hpi.

mutant and *RNAi-1*, their transcripts were measured using quantitative real-time reverse transcription (qRT)-PCR analysis. The results indicate that the expression of all three *PR* genes in the inoculated leaves of wild-type plants showed greater induction following pathogen inoculation at 24 and 48 hpi, in comparison with the *acbp3* mutant and *RNAi-1* (Fig. 4B).

To determine the possible link in SA levels to the activated defense phenotype observed in *ACBP3-OEs* and *ACBP3-KOs*, we measured the SA contents using HPLC. As shown in Figure 5, the endogenous SA levels in *OE-1* and *OE-4* were elevated 1.5-fold in comparison with that of the wild type. In contrast, no significant difference was observed between *ACBP3-KOs* and the wild type (Fig. 5). Taken together, our observations suggest that *ACBP3* expression seems important for induction of the plant defense response.

#### Activated Expression of *PR* Genes and Enhanced Pathogen Resistance in *ACBP3-OEs* Are Dependent on NPR1

To determine whether the constitutively induced expression of *PR* genes (Fig. 2) and enhanced plant disease resistance (Fig. 3) in *ACBP3-OEs* are related to an activation in the NPR1- or COI1-mediated signaling pathway, the expression of *PR1*, *PR2*, and *PR5* in wild-type and *ACBP3 OE-1* plants as well as *OE-1* in combination with a *npr1-5* (Shah et al., 1999) or *coi1-2* (Xiao et al., 2004) background was subsequently examined. The *npr1-5* (Shah et al., 1999) and *coi1-2* (Xiao et al., 2004) mutants were used because they are deficient in SA and JA signaling, respectively (Xiao et al., 2010). Our results from qRT-PCR (Fig. 6A) showed elevated expression in all *PR* genes (*PR1*, *PR2*, and *PR5*) in *OE-1*. However, these *PR* genes were significantly suppressed in the *OE-1npr1-5* line when *OE-1* was combined with the *npr1-5* mutation. The *OE-1npr1-5* line now resembled the *npr1-5* single mutant (Fig. 6A).

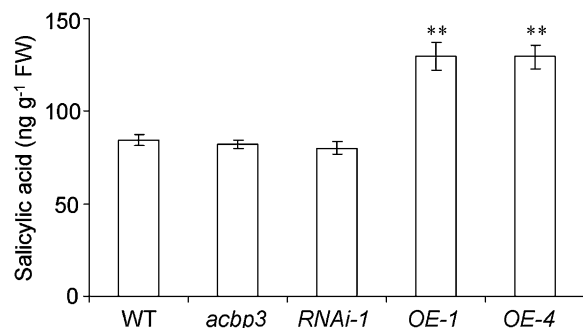


**Figure 5.** Endogenous SA contents in wild-type (WT), *ACBP3-OE*, and *ACBP3-KO* plants. Total SAs were extracted from leaf samples of 4-week-old wild-type, *ACBP3-OE* (*OE-1* and *OE-4*), and *ACBP3-KO* (*acbp3* and *RNAi-1*) plants and analyzed by HPLC. Data represent means of three samples from three independent plants. The experiment was repeated with similar results. FW, Fresh weight. \*\*  $P < 0.05$  by Student's *t* test.

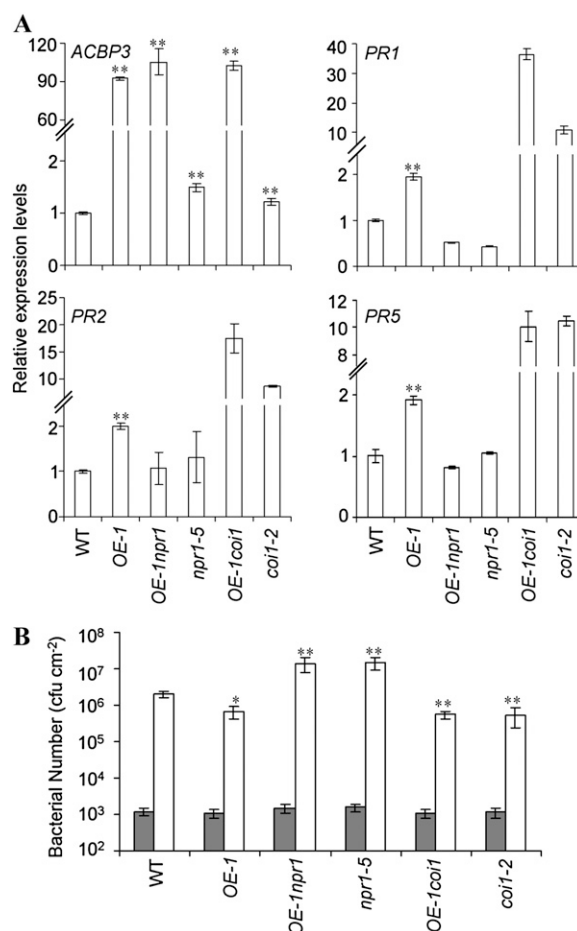


**Figure 6.** Activated *PR* gene expression and enhanced *P. syringae* resistance phenotypes in *ACBP3-OEs* are dependent on NPR1. A, qRT-PCR analyses of the expression levels of *ACBP3*, *PR1*, *PR2*, and *PR5* in 4-week-old wild-type (WT), *OE-1*, *OE-1npr1-5*, *npr1-5*, *OE-1coi1-2*, and *coi1-2* rosettes. Expression levels for each gene in all genotypes were normalized to the wild type. \*\*  $P < 0.01$  by Student's *t* test. B, Bacterial counts in the wild type, *OE-1*, *OE-1npr1-5*, *npr1-5*, *OE-1coi1-2*, and *coi1-2* at 0 and 4 dai. Three-week-old plants were sprayed with bacterial suspension ( $OD_{600} = 0.01$ ), data points represent means of three replicates (each replicate was pooled with three leaf discs) taken from three independent plants, and bacterial counts were determined on a per cm<sup>2</sup> basis. The experiment was repeated with similar results. cfu, Colony-forming units. \*  $P < 0.05$ , \*\*  $P < 0.01$  by Student's *t* test.

Consistent with previous findings (Ren et al., 2008), our data also revealed that the expression of *PR* genes was significantly elevated in the *coi1* mutant in comparison with the wild type (Fig. 6A). Interestingly, the *PR1* and *PR2* genes showed an additive induced expression in the *OE-1coi1* double mutant (Fig. 6A), which may have resulted from a combination of *ACBP3* overexpression and the *coi1-2* mutation. Furthermore, measurement of bacterial counts in plants following *P. syringae* inoculation showed that the *OE-1npr1* plants no longer exhibited an enhanced resistance to *P. syringae* infection, similar to the *npr1-5* mutant (Fig. 6B). As in previous findings (Kloek et al., 2001), the *coi1-2* mutant was more resistant to *P. syringae* infec-



tion and the *OE-1coi1-2* double mutant mimicked the response of the *coi1-2* mutant (Fig. 6B). These findings demonstrate that the enhanced expression of *PR* genes and resistance to *P. syringae* in *ACBP3*-OEs are dependent on NPR1.

#### Response of *ACBP3*-OEs and *ACBP3*-KOs to *B. cinerea* Infection

To determine the response of *ACBP3* to the necrotrophic fungal pathogen *B. cinerea*, the detached rosette leaves from the wild type, *ACBP3*-OEs (*OE-1* and *OE-4*), and *ACBP3*-KOs (*acbp3* and *ACBP3-RNAi*) were inoculated with *Botrytis* spores. As shown in Figure 7, the necrotic spots at the sites of inoculation were evident in wild-type leaves at 2 dai, and necroses in *ACBP3*-OE lines were more severe than in the wild type (Fig. 7A). In contrast, the spots in *ACBP3*-KOs were restricted (Fig. 7A). Similar results were observed by spraying *Botrytis* suspension (concentration of  $2 \times 10^5$  spores  $\text{mL}^{-1}$ ) onto wild-type, *ACBP3*-OE, and *ACBP3*-KO plants (Fig. 7B). At 7 dai, chlorosis and necrosis were evident in most rosette leaves of OE lines, but those of KO lines were relatively unaffected in comparison with the wild type (Fig. 7B), suggesting that *ACBP3*-OEs were more susceptible than *ACBP3*-KOs to *Botrytis* infection.

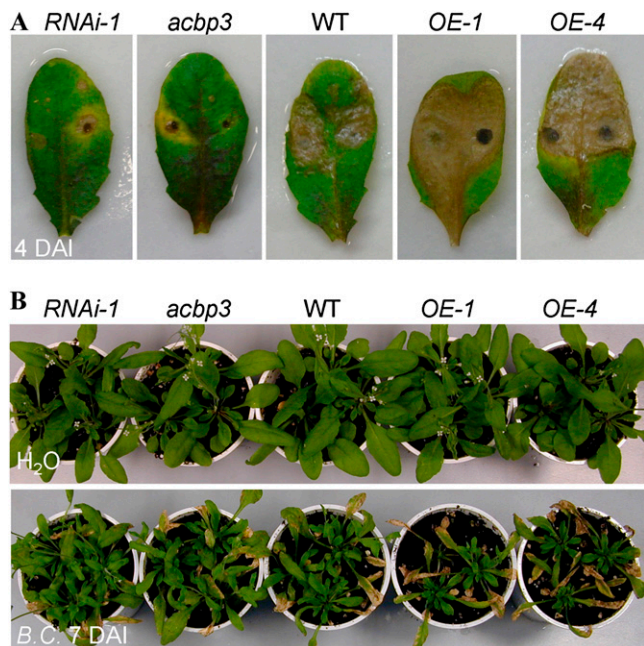


**Figure 7.** Response of *ACBP3*-OEs and *ACBP3*-KOs to *B. cinerea* infection. A, Representative rosettes of 3-week-old wild-type (WT), *ACBP3*-KO (*acbp3* and *ACBP3-RNAi*), and *ACBP3*-OE (*OE-1* and *OE-4*) plants showing disease manifestation after inoculation (by  $10\text{-}\mu\text{L}$  dotting using  $1 \times 10^5$  spores  $\text{mL}^{-1}$  suspension) with the fungus *B. cinerea*. Photographs were taken at 4 dai. B, Phenotypes of 3-week-old wild type, *ACBP3*-KO (*acbp3* and *ACBP3-RNAi*), and *ACBP3*-OE (*OE-1* and *OE-4*) plants sprayed with the pathogen *B. cinerea* ( $2 \times 10^5$  spores  $\text{mL}^{-1}$ ) or with water as a control ( $\text{H}_2\text{O}$ ) and photographed at 7 dai. The experiments were repeated with similar results.

#### The *ACBP3*-GFP Protein Is Degraded upon Pathogen Infection, and Inoculation of Intracellular Fluids from *ACBP3*-OE Plants Activates the Expression of *PR* Genes (*PR1* and *PR2*)

To investigate further the molecular mechanism of *ACBP3* in the plant defense response, an *ACBP3*-GFP construct was generated using the pBI-GFP plasmid (Xiao et al., 2008b) to facilitate tracking *ACBP3* following pathogen infection. The resultant plasmid was used to produce transgenic plants expressing *ACBP3*-GFP (Xiao et al., 2010) that were verified by confocal microscopy before being subjected to *P. syringae* DC3000 infection. Consistent with our previous reports (Leung et al., 2006; Xiao et al., 2010), *ACBP3*-GFP was confirmed to be localized to the apoplast and the endomembranes in the primary root of *ACBP3*-GFP transgenic plants (data not shown). Confocal microscopy revealed further that after *P. syringae* infection, *ACBP3*-GFP showed either altered localization (possibly to the endoplasmic reticulum or vesicles) or degradation at 72 h in leaf epidermal cells (Fig. 8B) and at 30 min in primary root cells (Fig. 8D). Such changes were not seen in leaf or root following control treatment using  $\text{MgCl}_2$  (Fig. 8, A and C, respectively).

Furthermore, when western-blot analysis was carried out using intracellular fluids (IFs) from *ACBP3*-GFP rosettes infected with *P. syringae*, the *ACBP3*-GFP protein appeared to be subject to degradation in samples taken at 48 and 72 h post infection (Fig. 8E). It is noted that relatively weaker signals were detected with full-length *ACBP3*-GFP bands (Fig. 8E, arrow), while GFP-degraded forms appeared much stronger (Fig. 8E, asterisk), perhaps arising from differences in anti-GFP antibody specificities to *ACBP3*-GFP fusion protein and the GFP domain alone. When the IF extracted from uninfected *ACBP3 OE-1* plants and *P. syringae*-infected *ACBP3 OE-1* plants were inoculated on wild-type rosettes, the expression of *PR1* and *PR2* mRNAs was induced in the inoculated (local) rosette leaves but not in uninfected (systemic) rosette leaves (Fig. 8F). *PR1* and *PR2* mRNAs seemed to be more highly expressed when IF was extracted from the infected *ACBP3 OE-1* plants than the uninfected plants. As a control, the use of wild-type IF did not induce *PR* gene expression in both local and systemic leaves (Fig. 8F).

#### Microarray Analyses of *ACBP3 OE-1*

To establish further the potential links between the molecular function of *ACBP3* and other pathways, we performed microarray analysis on the wild type and *ACBP3 OE-1*. The expression of 54 genes was observed to be up-regulated in *OE-1* plants (Supplemental Table S1). Following functional classification, most (21) genes were found to be associated with biotic/abiotic stresses and leaf senescence. Consistent with the results of Figure 2, the expression of pathogenesis-related genes, including *PR1*, *PR2*, and *PR5*, in *OE-1* showed

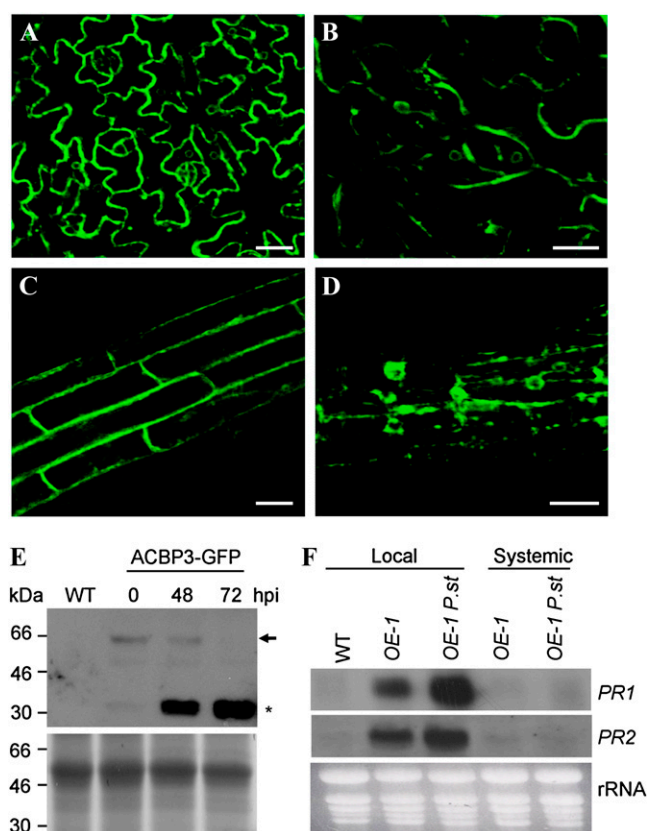


**Figure 8.** Effect of *P. syringae* DC3000 infection on ACBP3-GFP. A to D, Change in localization of the ACBP3-GFP fusion protein in transgenic Arabidopsis after *P. syringae* treatment. A and B, Confocal images showing leaf epidermal cells of 3-week-old ACBP3-GFP transgenic plants at 72 h following inoculation with 10 mM MgCl<sub>2</sub> (A) or syringe-infiltrated *P. syringae* DC3000 (10<sup>6</sup> colony-forming units mL<sup>-1</sup>; B). Bars = 20 μm. C and D, Confocal images showing primary root cells of 1-week-old ACBP3-GFP transgenic plants treated with 10 mM MgCl<sub>2</sub> (C) or with *P. syringae* DC3000 (10<sup>6</sup> colony-forming units mL<sup>-1</sup>) for 30 min (D). Bars = 20 μm. E, Western-blot analysis using GFP-specific antibodies of IFs from ACBP3-GFP transgenic plants infected with *P. syringae* DC3000 at 0, 48, and 72 h. The arrow indicates the ACBP3-GFP fusion protein, and the asterisk shows degraded protein derivatives. At bottom is an identically loaded gel stained with Coomassie blue. F, Inoculation of IF from OE-1 plants activates the expression of PR1 and PR2 in wild-type (WT) Arabidopsis. IFs extracted from wild-type, uninfected, and *P. syringae*-infected OE-1 (OE-1 P.st.) plants were inoculated on wild-type rosettes. OE-1 was infected with *P. syringae* DC3000 for 24 h. The inoculated (local) and systemic rosette leaves were harvested at 24 hpi for total RNA isolation. PR1 and PR2 expression was analyzed by RNA gel blotting using DIG-labeled cDNA probes. At bottom is an ethidium bromide-stained gel before blotting showing rRNA bands. The experiments were repeated with similar results.

increases (2.7-, 2.1-, and 2.0-fold, respectively) when compared with the wild type. Another defense-related gene that was up-regulated more than 2.0-fold (2.8-fold increase) was FLAVIN-DEPENDENT MONOOXYGENASE1 (FMO1; Bartsch et al., 2006). The expression of YELLOW LEAF-SPECIFIC GENE9 (YSL9; Yoshida et al., 2001) and SENESCENCE-ASSOCIATED GENE13

(SAG13; Miller et al., 1999), two well-known senescence-associated marker genes, increased 3.3- and 4.6-fold, respectively, confirming ACBP3 function in leaf senescence (Xiao et al., 2010). Furthermore, the expression of the *P. syringae* *avrRpt2*-inducible gene *AIG1* (Reuber and Ausubel, 1996) and *KTI1*, encoding a trypsin inhibitor in modulating PCD in plant-pathogen interactions (Li et al., 2008b), showed 3.9- and 4.4-fold increases, respectively (Supplemental Table S1).

Twelve genes related to stress responses, including oxidative stress, heat, Glc stress, wounding, and heavy metal stress, were up-regulated in OE-1 (Supplemental Table S1). In particular, the expression of ARABIDOPSIS THALIANA PLEIOTROPIC DRUG RESISTANCE12 (*AtPDR12*) increased 2.0-fold. Since *AtPDR12* mRNA is induced by lead [Pb(II)] treatment in both roots and shoots (Lee et al., 2005) and overexpression of *AtPDR12* conferred resistance to Pb(II), the ACBP3-OE plant may possibly show enhanced tolerance to Pb(II); this would be tested in the future given that ACBP1-overexpressors are Pb(II) tolerant (Xiao et al., 2008a) and that human ACBP has been reported to be a molecular target for Pb(II) (Smith et al., 1998). Another stress-related up-regulated gene in OE-1 is At1g28480, which encodes a member of the glutaredoxin family, GRX480, that is known to interact with TGA transcription factors and suppress the transcription of JA-responsive *PDF1.2* (Ndamukong et al., 2007). This finding is consistent with our results in northern-blot analysis showing the down-regulation of *PDF1.2* in ACBP3-OEs (Fig. 2A).

In addition, 15 genes related to metabolism, nine genes in transcription, transportation, and signaling, and eight genes of unknown function showed more than 2-fold up-regulation in OE-1 (Supplemental Table S1). In contrast to the 54 up-regulated genes, only 14 genes were down-regulated in OE-1 (Supplemental Table S2). Interestingly, most of these have been predicted to be localized in the extracellular space and many have unknown functions, while some (At1g57750, At1g66850, At1g58430, and At2g42990) are likely associated with lipid metabolism.

qRT-PCR was carried out further on ACBP3-OEs to validate the microarray data. The results of the increased expression of biotic- or abiotic stress-related genes (*PR1*, *PR5*, *AIG1*, *KTI1*, *GRX480*, *PR2*, *FMO1*, and *AtPDR12*) or senescence-associated genes (*SAG13* and *YSL9*) in ACBP3-OEs (OE-1 and OE-4) support the microarray results (Fig. 9). Similarly, the down-regulation of genes corresponding to At1g57750, At5g37940, and At5g07550 was confirmed by qRT-PCR (Fig. 9). The differences in fold change of some genes, such as *AIG1*, *KTI1*, *FMO1*, and *YSL9* in OE-1, between the microarray data and qRT-PCR results may possibly have arisen from differences in the developmental stages of the plant samples used in the two analyses. Taken together, our findings herein suggest that Arabidopsis ACBP3 has diverse functions in both plant development and the protection of plants from biotic or abiotic stress.

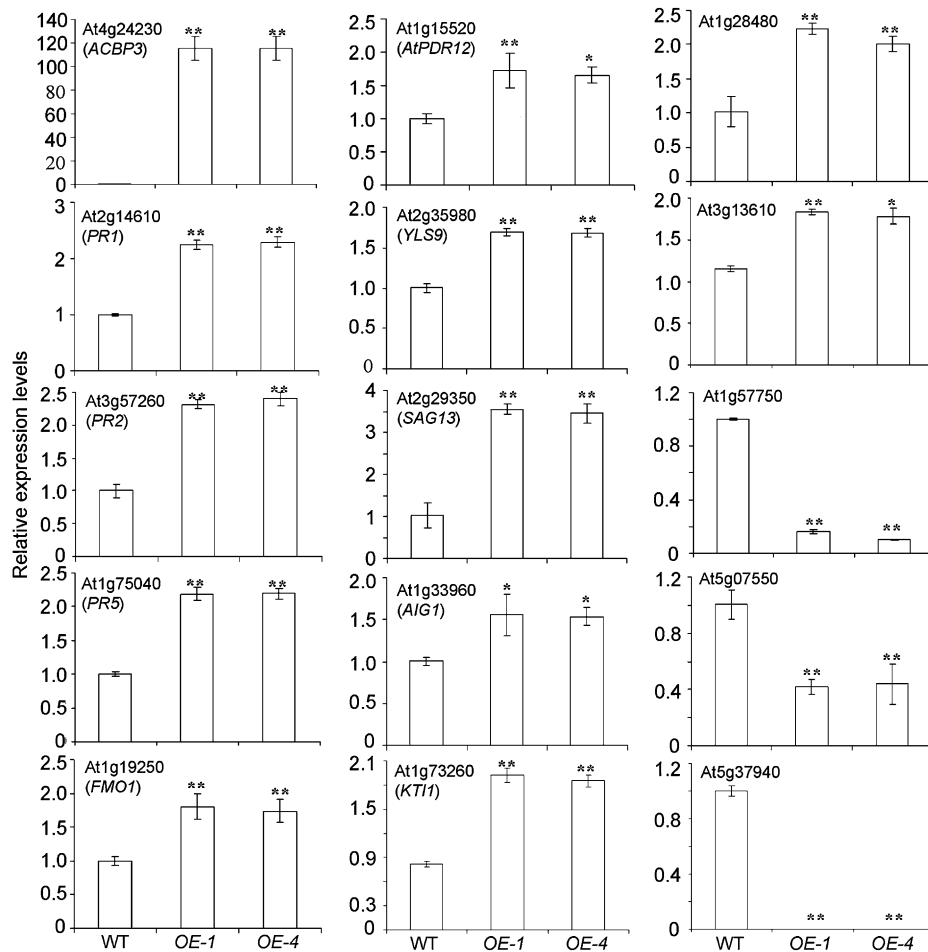


**Figure 9.** Real-time qRT-PCR analyses validating the relative expression of selected up-regulated genes (boldface in Supplemental Table S1) or down-regulated genes (boldface in Supplemental Table S2) in *OE-1* and *OE-4* in comparison with the wild type. The up-regulated genes analyzed were **At2g14610** (*PR1*), **At3g57260** (*PR2*), **At1g75040** (*PR5*), **At1g19250** (*FMO1*), **At1g15520** (*AtPDR12*), **At2g35980** (*YELLOW LEAF-SPECIFIC GENE9* [*YLS9*]), **At2g29350** (*SAG13*), **At1g33960** (*avrRpt2-INDUCIBLE GENE1* [*AIG1*]), **At1g73260** (*KUNITZ TRYPSIN INHIBITOR1* [*KT11*]), **At1g28480** (encodes *GRX480*, which interacts with TGA factors and suppresses JA-responsive *PDF1.2* transcription), and **At3g13610** [encodes 2-oxoglutarate and Fe (II)-dependent oxygenase superfamily protein]. The down-regulated genes analyzed were **At1g57750** (encodes *CYP96A15*, a mid-chain alkane hydroxylase, involved in cuticular wax biosynthesis), **At5g07550** (encodes a member of the oleosin-like protein family), and **At5g37940** (encodes a zinc-binding dehydrogenase family protein). The expression of *ACBP3* (**At4g24230**) was used as a positive control. All of gene descriptions are obtained from The Arabidopsis Information Resource (www.Arabidopsis.org). Expression levels for each gene in *OE-1* and *OE-4* were normalized to the wild type. \*  $P < 0.05$ , \*\*  $P < 0.01$ .

## DISCUSSION

We have previously demonstrated that Arabidopsis *ACBP3* plays an important role in regulating leaf senescence by modulation of *ATG8* protein stability and in autophagosome formation in the autophagy pathway (Xiao et al., 2010; Xiao and Chye, 2011). In this study, the function of Arabidopsis *ACBP3* in plant defense was established by phenotypic analyses of *ACBP3-OE* and *ACBP3-KO* lines in response to biotrophic and necrotrophic pathogen infections as well as by using bioinformatics data showing downstream up-regulated expression of many biotic and abiotic stress-related genes in an *ACBP3-OE* line in comparison with the wild type.

Many secondary signal molecules, including SA, ethylene, and JA, produced during plant-pathogen interactions initiate various defense responses in plants. Recently, the roles of lipids and lipid-related proteins in plant disease resistance as well as plant-microbe interactions have been extensively studied (Shah, 2005). Among them, JA and its derivatives are well-studied lipid-derived signal molecules of plants in response to wounding during herbivory or pathogen infection (Shah, 2005). However, by analyses of *ACBP3-OE* in SA signaling mutant *npr1* (Shah et al., 1999) and JA perception mutant *coi1* (Xiao et al., 2004) backgrounds, our data suggest that the *ACBP3*-mediated defense response relies on the *NPR1*-mediated (not the *COI1*-



mediated) signaling pathway, indicating a possible role for lipid-derived signals in JA-independent early events in the plant response to biotic and/or abiotic stresses. There is mounting evidence that supports the involvement of genes affecting membrane lipid biosynthesis in plant defense. For example, the Arabidopsis *FATTY ACID DESATURASE7*, *SUPPRESSOR OF FATTY ACID DESATURASE DEFICIENCY1* (*SFD1*), and *SFD2* genes are essential for SA-dependent, but not JA-dependent, systemic acquired resistance (Nandi et al., 2004; Chaturvedi et al., 2008), suggesting that although membrane lipids provide fatty acid for JA synthesis, an intact JA signaling pathway is not essential for the lipid-associated plant defense pathway. Although the expression of *ACBP3* was induced by both exogenous JA and SA treatments, *ACBP3-OE* plants exhibited constitutive *PR* gene expression and the enhancement in *P. syringae* resistance was completely dependent on *NPR1*. The rosette leaves of *ACBP3-OEs* were characterized by cell death that was accompanied by the demonstration of an enhanced resistance to the biotrophic pathogen *P. syringae*. In contrast, these *OE* lines were more susceptible to the necrotrophic pathogen *B. cinerea*. Given the fact that mutual suppression cross talk occurs between the SA and JA signaling pathways, our observations are not unexpected, because such phenotypes have been frequently seen in many other mutants of SA-dependent defense genes (Glazebrook, 2005). However, in contrast to the *NPR1*-dependent *PR* gene expression and defense response in *ACBP3-OEs*, our results have revealed that the SA-induced expression pattern of *ACBP3* was unaffected in the *npr1-1* mutant. Instead, its expression level was somewhat up-regulated by SA treatment in the *npr1-1* mutant, suggesting that *NPR1* is a negative regulator of *ACBP3* gene expression. Given the findings that SA levels usually increase in *npr1* mutants, a negative feedback loop for *NPR1* in regulating SA synthesis through *ISOCHORISMATE SYNTHASE1* has been suggested (Delaney et al., 1995; Shah et al., 1997; Shah, 2003). Therefore, up-regulation of *ACBP3* in the *npr1-1* mutant can be explained by an elevation of endogenous SA, and it seems that *ACBP3* involvement in plant defense could be associated with *NPR1* protein function.

Generally, the delivery of endogenous proteins to the apoplastic space or the movement of proteins between plant cells occurs either via the secretory pathway or the plasmodesmata (Rojo et al., 2002). Using autofluorescence-tagged *ACBP3* fusions, *ACBP3* was observed to be extracellularly targeted and the signal peptide in *ACBP3* has been proven sufficient for extracellular targeting (Leung et al., 2006; Xiao et al., 2010), suggesting that *ACBP3* is distinctive in its localization in comparison with the five other *ACBPs*. The colocalization of autofluorescence-tagged *ACBP3* with fluorescence-labeled Golgi/endoplasmic reticulum complex and vesicles supports an extracellular localization of *ACBP3* in association with the secretory pathway (Xiao et al., 2010). Similar to *ACBP3*, many other apoplast proteins, such as *CONSTITUTIVE DIS-*

*EASE RESISTANCE1* (*CDR1*) and *DEFECTIVE IN INDUCED RESISTANCE1* (*DIR1*) in Arabidopsis, are known to be associated with either local or systemic defense responses (Maldonado et al., 2002; Xia et al., 2004). Arabidopsis *CDR1* encodes an apoplastic aspartic protease and *CDR1*-overexpression lines display enhanced resistance to virulent *P. syringae*, while its antisense down-regulated transgenic lines are more susceptible, suggesting that *CDR1* or *CDR1*-mediated peptide signals are essential for the activation of a SA-dependent plant defense response (Xia et al., 2004). The *DIR1* gene encodes a putative lipid transfer protein, indicating that lipid-based molecules can act as mobile signals in plant systemic acquired resistance (Maldonado et al., 2002). Given that *DIR1* is an extracellular localized protein, this would be consistent with its role in signaling and implies that plasma membrane receptors participate in *DIR1*-mediated systemic acquired resistance (Maldonado et al., 2002). The findings presented in this study indicate a role for *ACBP3* in plant resistance against the bacterial pathogen, strengthening further the hypothesis of Maldonado et al. (2002) that extracellular lipid signaling may be an important signal mediator or transducer of the plant defense response.

The presence of a transmembrane domain in the *ACBP3* N terminus and its membrane association from studies on subcellular fractionation and confocal microscopy (Xiao et al., 2010) suggest that, unlike other apoplast-localized proteins, *ACBP3* may have dual functions in plant development and defense. Indeed, other than its role in the regulation of autophagy-mediated leaf senescence, we found that its expression is induced in response to external environmental cues, including fungal and bacterial pathogens. Interestingly, recent studies on the autophagy proteins (*ATGs*) have already linked the autophagy pathway to the SA signaling-dependent plant innate immunity-associated *PCD* (Liu et al., 2005; Hofius et al., 2009; Yoshimoto et al., 2009). Our observations on the constitutive expression of *PR* genes and the *PCD* phenotypes of *ACBP3-OEs* that resemble those of *atg2* and *atg5* mutants in Arabidopsis (Yoshimoto et al., 2009) support a negative role for autophagy in the regulation of *PCD* in plants. However, unlike the enhanced resistance of *ACBP3-OEs* to *P. syringae* DC3000, the *atg5* mutants did not significantly affect the growth of *P. syringae* expressing *avrRPM1* (Yoshimoto et al., 2009). Recent evidence from two independent groups has indicated that the *atg5*, *atg7*, *atg10*, and *atg18a* mutants are more susceptible to the necrotrophic pathogen *B. cinerea* (Lai et al., 2011; Lenz et al., 2011) and that the *atg5*, *atg10*, and *atg18a* mutants are more resistant against virulent *P. syringae* DC3000 infection and accumulate higher levels of endogenous SA (Lenz et al., 2011). These findings are consistent with our observations on the *ACBP3-OE* lines and strongly suggest that the *ACBP3*-associated differential regulation of the plant response to necrotrophic and biotrophic pathogenic infections is possibly mediated

by the autophagy pathway. On the other hand, given our observations of PCD and H<sub>2</sub>O<sub>2</sub> accumulation in the premature leaves of *ACBP3-OEs*, the constitutive defense phenotype in *ACBP3-OE* lines could be due to cell death resulting from an elevation in H<sub>2</sub>O<sub>2</sub>. Nonetheless, it is also very likely that other associated components (e.g. extracellular lipid signaling) representing autophagy-independent pathways coexist in *ACBP3-OEs* that can trigger a bacterial resistance phenotype, possibly due to the apoplastic localization of ACBP3.

Given that recombinant ACBP3 binds arachidonyl-CoA esters with high affinity (Leung et al., 2006) and that AA is a well-known lipophilic molecule of fungal origin with elicitor activity (Smith, 1996), ACBP3 may possibly be involved in pathogen recognition by binding lipid molecules secreted by bacterial or fungal pathogens or other pathogen-derived signals released during infection for subsequent transmission into the plant cell that would culminate in strengthening existing defenses and trigger other defense pathways. This idea is supported by the rapid inducible expression of *ACBP3* mRNA in response to AA treatment. However, in contrast to rapid mRNA induction, analysis of the ACBP3-GFP fusion protein revealed that it is quickly degraded upon *P. syringae* DC3000 infection. The observation of ACBP3-GFP degradation upon pathogen invasion raises a possible link between ACBP3-mediated lipid signals and CDR1-mediated peptide signals (Xia et al., 2004). One likely explanation in plant-pathogen recognition mediated by ACBP3 may involve its binding to pathogen-secreted lipids (e.g. AA), after which the ACBP3-lipid complex is rapidly degraded by the apoplast protease (possibly CDR1) for initiation of the inducible plant disease resistance. Similar to that of CDR1 overexpressors, the activated expression of *PR* genes in response to the inoculation of IFs extracted from *ACBP3-OEs* is most likely induced by the SA pathway. On the other hand, the ubiquitination-associated proteins have recently been identified to play important roles in the plant's response to biotic and abiotic stresses (Zeng et al., 2006). Hence, Arabidopsis ACBP3 can also be targeted by the pathogen-derived E3 ubiquitin ligase for degradation during plant-microbe interaction (Zeng et al., 2006).

The results presented here provide strong evidence of an important role for Arabidopsis ACBP3 in the plant defense response. Taken together with findings reported in our previous studies (Leung et al., 2006; Xiao et al., 2010; Xiao and Chye, 2009, 2011), we propose that ACBP3 is likely involved in both NPR1-dependent bacterial pathogen resistance (by its ability to regulate the autophagy-mediated PCD pathway) and the lipid signaling pathway. The latter may result in a contribution of enhanced recognition of biotrophic and necrotrophic pathogens during the early stages of plant-microbial interaction. In both cases, activated *ACBP3* expression will consequently trigger the plant defense system by enhancing the expression of *PR* genes as well as other defense-related genes. Future work on downstream up- or down-regulated genes in

*ACBP3-OE* lines is expected to improve further our understanding of this ACBP in both biotic and abiotic stress pathways.

## MATERIALS AND METHODS

### Plant Materials, Growth Conditions, and Treatments

All Arabidopsis (*Arabidopsis thaliana*) wild-type (ecotype Col-0), *acbp3*, *ACBP3-RNAi*, and *ACBP3-OE* (Xiao et al., 2010) lines were grown under light/dark cycles in conditions of 16 h of light, 23°C/8 h of dark, 21°C. For Arabidopsis treatments in RNA gel-blot experiments, seedlings were grown on Murashige and Skoog (1962; MS) medium in continuous light for 2 to 3 weeks and then treated with 10 μM AA (Sigma-Aldrich), 1 mM ACC (Sigma-Aldrich), 100 μM MeJA (Sigma-Aldrich), 1 mM SA (Sigma-Aldrich), or water (control). Plant samples were collected at the time points indicated in the figures.

Arabidopsis wild-type and *OE-1* plants used for microarray gene expression analysis were germinated on MS. The seeds were first placed at 4°C for 2 d and then cultivated in 16-h-light/8-h-dark cycles for 1 week in a tissue culture room. The MS-grown wild-type and *OE-1* plants were planted in soil for another 2 weeks in a growth chamber under similar growth conditions (16 h of light, 23°C/8 h of dark, 21°C). After genotyping, rosette leaves from 3-week-old wild-type and *OE-1* plants were collected, immediately frozen in liquid nitrogen, and stored at -80°C until use.

### Culture of Pathogen and Inoculation of Plants

The bacterial strain *Pseudomonas syringae* pv *tomato* DC3000 (ATCC No. BBA-871) and fungus strain *Botrytis cinerea* (ATCC No. 11542) were obtained from the American Type Culture Collection. Bacteria were grown on King's B medium supplemented with rifampicin (50 μg mL<sup>-1</sup>) and incubated at 25°C. One day before the assay, a single bacterial colony inoculated in King's B liquid medium containing rifampicin (50 μg mL<sup>-1</sup>) was cultured at 28°C overnight with shaking until midlog growth phase (optical density at 600 nm [OD<sub>600</sub>] = 0.134) was obtained. Cells were then collected by centrifugation at 4,000g for 7 min and resuspended in 5 mL of 10 mM MgCl<sub>2</sub>. Rosette leaves of 3-week-old plants were sprayed with bacterial suspensions (OD<sub>600</sub> = 0.01 in 10 mM MgCl<sub>2</sub>). For RNA gel-blot analyses, plant samples were collected at 0, 12, 24, and 48 hpi. For phenotypic observations, plants were photographed at 0 and 4 dai. Determination of in planta bacterial growth was performed as described (Cao et al., 1994; Shah et al., 1997). Three independently infected leaves were used for the wild-type and other plant genotypes, and three leaf discs of the same size (0.6 cm in diameter and area of 0.28 cm<sup>2</sup>) were taken from each leaf using a hole puncher and pooled as one replicate. The leaf discs were washed three times with distilled water and homogenized in 10 mM MgCl<sub>2</sub> using a plastic pestle. Bacterial growth numbers were determined by plating appropriate dilutions from each sample in King's B medium containing rifampicin (50 μg mL<sup>-1</sup>). For defense gene expression analyses, the rosettes of 3-week-old plants were syringe infiltrated with bacterial suspensions (OD<sub>600</sub> = 0.001 in 10 mM MgCl<sub>2</sub>), and samples were collected at the times indicated in the figures.

The fungus *B. cinerea* was cultured on a potato dextrose agar (BD Difco; catalog no. 213400) agar plate and incubated at room temperature. Collection of conidia and plant inoculation were performed according to previous protocols (Xiao et al., 2004; Li et al., 2008a). The rosettes of 3-week-old Arabidopsis were inoculated with the fungus *B. cinerea* by either inoculating a 10-μL droplet of spore suspension (1 × 10<sup>5</sup> spores mL<sup>-1</sup>) or spraying a spore suspension (2 × 10<sup>5</sup> spores mL<sup>-1</sup>) in water containing 1% Glc. Water containing 1% Glc was used as a control. After inoculation, the plants were placed in a growth chamber with high humidity (100%) at 22°C under growth conditions of a 16-h-light/8-h-dark photoperiod. Plant samples were photographed at 4 dai (for dotting inoculation) and 7 dai (for spraying inoculation). Samples were collected at 0, 12, 24, and 48 hpi for RNA gel-blot analyses.

### RNA Gel-Blot Analysis

Total RNA extraction and RNA gel-blot analysis were carried out as described previously (Xiao et al., 2008a). Briefly, 30 μg of total RNA was separated on a 1.5% agarose gel containing 6% formaldehyde and transferred to Hybond N membranes (Amersham). The gene-specific primers used to generate cDNA probes are summarized in Supplemental Table S3. The cDNA fragments were labeled with the PCR Digoxigenin Probe Synthesis Kit

according to the manufacturer's instructions (Roche), and the wild-type first-strand cDNAs were used as templates. Hybridization and detection were performed according to standard procedures (Roche). Blots were washed under conditions of high stringency ( $2\times$  SSC, 0.1% SDS for  $2\times$  15 min at room temperature;  $0.5\times$  SSC, 0.1% SDS for  $2\times$  15 min at 68°C;  $0.1\times$  SSC, 0.1% SDS for  $2\times$  15 min at 68°C).

For the experiment concerning *ACBP3-OE* IF induction of *PR* gene expression, IFs extracted from wild-type and *ACBP3 OE-1* plants as well as from *ACBP3 OE-1* plants infected for 24 h with *P. syringae* DC3000 ( $10^6$  colony-forming units  $\text{mL}^{-1}$ ) were inoculated on wild-type (Col-0) rosettes. Samples were collected from inoculated local leaves and uninoculated systemic leaves for RNA gel-blot analyses.

## Trypan Blue and DAB Staining

Trypan blue staining (Alvarez et al., 1998) and DAB staining (Thordal-Christensen et al., 1997) were carried out as described previously with minor modifications. For trypan blue staining, rosettes from 4-week-old wild-type and *ACBP3-OE* plants were boiled for 1 min in trypan blue staining buffer (12.5% phenol, 12.5% glycerol, 12.5% lactic acid, 48% ethanol, and 0.025% trypan blue) and incubated for 10 min at room temperature, followed by destaining (five times) in 70% chloral hydrate. For DAB staining, rosettes from 4-week-old wild-type and *ACBP3-OE* plants were cut and placed in 1 mg  $\text{mL}^{-1}$  DAB solution (pH 3.8) overnight (about 8 h) at room temperature and subsequently cleared in 96% boiling ethanol for 10 min.

## qRT-PCR

Total RNA (3  $\mu\text{g}$ ) extracted using TRIzol reagent was reverse transcribed into cDNA by using the SuperScript First-Strand Synthesis System (Invitrogen; catalog no. 12371-019) according to the manufacturer's instructions. PCR was conducted on a StepOne Plus real-time PCR system using SYBR Green Mix (Applied Biosystems). The conditions for qRT-PCR were as follows: initial denaturation at 95°C (10 min) followed by 40 cycles of 95°C (15 s) and 56°C (1 min). For each reaction, three experimental replicates were obtained using primer pairs specific to the gene of interest and an Arabidopsis ACTIN internal control as listed in Supplemental Table S4. The relative expression level of each investigated gene was normalized to that of the ACTIN control by subtracting the threshold cycle value of ACTIN from that of the investigated gene. Fold change in expression was calculated according to the comparative threshold cycle method (Schmittgen and Livak, 2008). The data shown in this study represent means  $\pm$  SD of two independent experiments.

## SA Measurement

SA was extracted from 0.3 to 0.5 g of 4-week-old leaves of wild-type, *ACBP3-OE*, and *ACBP3-KO* plants according to Morita-Yamamuro et al. (2005). After extraction, the dried residues were resuspended in 50% methanol and analyzed by HPLC with a fluorescent detector set at excitation = 295 nm and emission = 370 nm.

## Laser-Scanning Confocal Microscopy

For the analysis of ACBP3-GFP localization before and after pathogen infection, an inverted confocal laser-scanning microscope (Zeiss LSM 510) equipped with helium/neon lasers and multitracking was used as described previously (Xiao et al., 2010). GFP fluorescence, excited at 488 nm, was emitted through a primary dichroic filter (UV/488/543), a secondary dichroic filter (545 nm), and BP505-530 nm emission filters to the photomultiplier tube detector. LSM 510 software (Zeiss) was used to process the images obtained.

## IF Extraction and Western-Blot Analysis

The IFs from Arabidopsis were extracted according to Xia et al. (2004) with minor modifications. Plant leaves were harvested and completely immersed in extraction buffer (100 mM Tris-HCl, pH 7.5, 5 mM  $\text{MgCl}_2$ , and 2 mM EDTA). Leaves were infiltrated under vacuum (720 mm Hg) for 2 min followed by rapid release. Infiltration was repeated twice. Subsequently, the leaves were removed from the extraction buffer and placed between two absorbent papers to blot off the surface buffer. Leaves were then placed in a 50-mL Falcon tube containing a supported mesh for the separation and recovery of the IFs from the leaves. IFs

were obtained from the infiltrated leaves by centrifugation at 3,000g for 15 min. Total protein was extracted by homogenizing 3-week-old wild-type Arabidopsis rosettes according to Xiao et al. (2008b). Proteins were separated by 12% SDS-PAGE and subsequently transferred onto Hybond-C membranes (Amersham) using a Trans-Blot cell (Bio-Rad). The membranes were blocked for 2 h in  $1\times$  Tris-buffered saline plus 0.05% Tween 20 with 5% nonfat milk and incubated for another 2 h with anti-GFP (Invitrogen; 1:3,000) primary antibodies. The blots were washed three times with Tris-buffered saline plus 0.05% Tween 20 and then incubated for 1 h with secondary antibody. The ECL Western Blotting Detection Kit (Amersham) was used following the manufacturer's instructions for detection of cross-reacting bands.

## Microarray Analysis

Total RNA was extracted and purified using the RNeasy Mini Kit (Qiagen) with on-column DNase digestion according to the manufacturer's instructions. The RNA quality and quantity were examined with the Bioanalyzer 2100 (Agilent Technologies) and MOPS-formaldehyde agarose gels. Each sample contains three biological replicates, and each replicate consists of a pool of RNA from three plants. Affymetrix ATH1 arrays were used for hybridization. GeneSpring GX software (Agilent) and the MAS5 algorithm were used in data collection and normalization. Welch's approximate *t* test statistical analysis was followed by fold change and significance analysis between *OE-1* and wild-type samples. Significantly differentially regulated genes were subsequently identified using Benjamini-Hochberg multiple testing correction, with  $P < 0.05$  and change  $> 2.0$ -fold in *OE-1* samples when compared with wild type samples considered as cutoff values. Gene functional classification was analyzed using online software DAVID tools (<http://david.abcc.ncifcrf.gov/>) and MapMan (<http://ppdb.tc.cornell.edu/dbsearch/searchacc.aspx>) according to the Gene Ontology consortium (<http://amigo.geneontology.org/cgi-bin/amigo/go.cgi>).

Sequence data from this article can be found in the GenBank/EMBL data libraries under accession numbers NM\_001084972 (*ACBP3*), NM\_127025 (*PR1*), NM\_115586 (*PR2*), NM\_106161 (*PR5*), and NM\_123809 (*PDF1.2*).

## Supplemental Data

The following materials are available in the online version of this article.

**Supplemental Table S1.** Genes up-regulated more than 2-fold in *ACBP3 OE-1*.

**Supplemental Table S2.** Genes down-regulated more than 2-fold in *ACBP3 OE-1*.

**Supplemental Table S3.** Sequences of gene-specific primers to generate cDNA probes for RNA gel-blot analyses.

**Supplemental Table S4.** Sequences of gene-specific primers for qRT-PCR.

Received March 23, 2011; accepted June 10, 2011; published June 13, 2011.

## LITERATURE CITED

- Alvarez ME, Pennell RI, Meijer PJ, Ishikawa A, Dixon RA, Lamb C (1998) Reactive oxygen intermediates mediate a systemic signal network in the establishment of plant immunity. *Cell* **92**: 773–784
- Bartsch M, Gobbato E, Bednarek P, Debey S, Schultze JL, Bautor J, Parker JE (2006) Salicylic acid-independent ENHANCED DISEASE SUSCEPTIBILITY1 signaling in *Arabidopsis* immunity and cell death is regulated by the monooxygenase FMO1 and the Nudix hydrolase NUDT7. *Plant Cell* **18**: 1038–1051
- Cao H, Bowling SA, Gordon AS, Dong X (1994) Characterization of an *Arabidopsis* mutant that is nonresponsive to inducers of systemic acquired resistance. *Plant Cell* **6**: 1583–1592
- Chaturvedi R, Krothapalli K, Makandar R, Nandi A, Sparks AA, Roth MR, Welti R, Shah J (2008) Plastid  $\omega$ 3-fatty acid desaturase-dependent accumulation of a systemic acquired resistance inducing activity in petiole exudates of *Arabidopsis thaliana* is independent of jasmonic acid. *Plant J* **54**: 106–117
- Chen QF, Xiao S, Chye ML (2008) Overexpression of the Arabidopsis

- 10-kilodalton acyl-coenzyme A-binding protein ACBP6 enhances freezing tolerance. *Plant Physiol* **148**: 304–315
- Chen QF, Xiao S, Qi WQ, Mishra G, Ma J, Wang M, Chye ML** (2010) The *Arabidopsis* *acbp1acbp2* double mutant lacking acyl-CoA-binding proteins ACBP1 and ACBP2 is embryo lethal. *New Phytol* **186**: 843–855
- Chye ML** (1998) *Arabidopsis* cDNA encoding a membrane-associated protein with an acyl-CoA binding domain. *Plant Mol Biol* **38**: 827–838
- Chye ML, Huang BQ, Zee SY** (1999) Isolation of a gene encoding *Arabidopsis* membrane-associated acyl-CoA binding protein and immunolocalization of its gene product. *Plant J* **18**: 205–214
- Chye ML, Li HY, Yung MH** (2000) Single amino acid substitutions at the acyl-CoA-binding domain interrupt [<sup>14</sup>C]palmitoyl-CoA binding of ACBP2, an *Arabidopsis* acyl-CoA-binding protein with ankyrin repeats. *Plant Mol Biol* **44**: 711–721
- Delaney TP, Friedrich L, Ryals JA** (1995) *Arabidopsis* signal transduction mutant defective in chemically and biologically induced disease resistance. *Proc Natl Acad Sci USA* **92**: 6602–6606
- Du ZY, Xiao S, Chen QF, Chye ML** (2010) Depletion of the membrane-associated acyl-coenzyme A-binding protein ACBP1 enhances the ability of cold acclimation in *Arabidopsis*. *Plant Physiol* **152**: 1585–1597
- Engeseth NJ, Pacovsky RS, Newman T, Ohlrogge JB** (1996) Characterization of an acyl-CoA-binding protein from *Arabidopsis thaliana*. *Arch Biochem Biophys* **331**: 55–62
- Faergeman NJ, Knudsen J** (2002) Acyl-CoA binding protein is an essential protein in mammalian cell lines. *Biochem J* **368**: 679–682
- Fan J, Liu J, Culty M, Papadopoulos V** (2010) Acyl-coenzyme A binding domain containing 3 (ACBD3; PAP7; GCP60): an emerging signaling molecule. *Prog Lipid Res* **49**: 218–234
- Gao W, Li HY, Xiao S, Chye ML** (2010) Acyl-CoA-binding protein 2 binds lysophospholipase 2 and lysoPC to promote tolerance to cadmium-induced oxidative stress in transgenic *Arabidopsis*. *Plant J* **62**: 989–1003
- Gao W, Xiao S, Li HY, Tsao SW, Chye ML** (2009) *Arabidopsis thaliana* acyl-CoA-binding protein ACBP2 interacts with heavy-metal-binding farnesylated protein AtFP6. *New Phytol* **181**: 89–102
- Glazebrook J** (2005) Contrasting mechanisms of defense against biotrophic and necrotrophic pathogens. *Annu Rev Phytopathol* **43**: 205–227
- Hofius D, Schultz-Larsen T, Joensen J, Tsitsigiannis DI, Petersen NH, Mattsson O, Jørgensen LB, Jones JD, Mundy J, Petersen M** (2009) Autophagic components contribute to hypersensitive cell death in *Arabidopsis*. *Cell* **137**: 773–783
- Kloek AP, Verbsky ML, Sharma SB, Schoelz JE, Vogel J, Klessig DF, Kunkel BN** (2001) Resistance to *Pseudomonas syringae* conferred by an *Arabidopsis thaliana* coronatine-insensitive (*coi1*) mutation occurs through two distinct mechanisms. *Plant J* **26**: 509–522
- Knudsen J, Neergaard TB, Gaigg B, Jensen MV, Hansen JK** (2000) Role of acyl-CoA binding protein in acyl-CoA metabolism and acyl-CoA-mediated cell signaling. *J Nutr (Suppl)* **130**: 294S–298S
- Lai Z, Wang F, Zheng Z, Fan B, Chen Z** (2011) A critical role of autophagy in plant resistance to necrotrophic fungal pathogens. *Plant J* **66**: 953–968
- Lee M, Lee K, Lee J, Noh EW, Lee Y** (2005) AtPDR12 contributes to lead resistance in *Arabidopsis*. *Plant Physiol* **138**: 827–836
- Lenz HD, Haller E, Melzer E, Kober K, Wurster K, Stahl M, Bassham DC, Vierstra RD, Parker JE, Bautor J, et al** (2011) Autophagy differentially controls plant basal immunity to biotrophic and necrotrophic pathogens. *Plant J* **66**: 818–830
- Leung KC, Li HY, Mishra G, Chye ML** (2004) ACBP4 and ACBP5, novel *Arabidopsis* acyl-CoA-binding proteins with kelch motifs that bind oleoyl-CoA. *Plant Mol Biol* **55**: 297–309
- Leung KC, Li HY, Xiao S, Tse MH, Chye ML** (2006) *Arabidopsis* ACBP3 is an extracellularly targeted acyl-CoA-binding protein. *Planta* **223**: 871–881
- Levine B, Klionsky DJ** (2004) Development by self-digestion: molecular mechanisms and biological functions of autophagy. *Dev Cell* **6**: 463–477
- Li HY, Chye ML** (2003) Membrane localization of *Arabidopsis* acyl-CoA binding protein ACBP2. *Plant Mol Biol* **51**: 483–492
- Li HY, Chye ML** (2004) *Arabidopsis* acyl-CoA-binding protein ACBP2 interacts with an ethylene-responsive element-binding protein, AtEBP, via its ankyrin repeats. *Plant Mol Biol* **54**: 233–243
- Li HY, Xiao S, Chye ML** (2008a) Ethylene- and pathogen-inducible *Arabidopsis* acyl-CoA-binding protein 4 interacts with an ethylene-responsive element binding protein. *J Exp Bot* **59**: 3997–4006
- Li J, Brader G, Palva ET** (2008b) Kunitz trypsin inhibitor: an antagonist of cell death triggered by phytopathogens and fumonisins b1 in *Arabidopsis*. *Mol Plant* **1**: 482–495
- Liu Y, Schiff M, Czymbek K, Tallóczy Z, Levine B, Dinesh-Kumar SP** (2005) Autophagy regulates programmed cell death during the plant innate immune response. *Cell* **121**: 567–577
- Maldonado AM, Doerner P, Dixon RA, Lamb CJ, Cameron RK** (2002) A putative lipid transfer protein involved in systemic resistance signalling in *Arabidopsis*. *Nature* **419**: 399–403
- Meng W, Su YCF, Saunders RMK, Chye ML** (2011) The rice acyl-CoA-binding protein gene family: phylogeny, expression and functional analysis. *New Phytol* **189**: 1170–1184
- Miller JD, Arteca RN, Pell EJ** (1999) Senescence-associated gene expression during ozone-induced leaf senescence in *Arabidopsis*. *Plant Physiol* **120**: 1015–1024
- Morita-Yamamoto C, Tsutsui T, Sato M, Yoshioka H, Tamaoki M, Ogawa D, Matsuura H, Yoshihara T, Ikeda A, Uyeda I, et al** (2005) The *Arabidopsis* gene *CAD1* controls programmed cell death in the plant immune system and encodes a protein containing a MACPF domain. *Plant Cell Physiol* **46**: 902–912
- Murashige T, Skoog F** (1962) A revised medium for rapid growth and bioassays with tobacco tissue cultures. *Physiol Plant* **15**: 473–497
- Nandi A, Welti R, Shah J** (2004) The *Arabidopsis thaliana* dihydroxyacetone phosphate reductase gene SUPPRESSOR OF FATTY ACID DESATURASE DEFICIENCY1 is required for glycerolipid metabolism and for the activation of systemic acquired resistance. *Plant Cell* **16**: 465–477
- Ndamukong I, Abdallat AA, Thurow C, Fode B, Zander M, Weigel R, Gatz C** (2007) SA-inducible *Arabidopsis* glutaredoxin interacts with TGA factors and suppresses JA-responsive PDF1.2 transcription. *Plant J* **50**: 128–139
- Ohsumi Y** (2001) Molecular dissection of autophagy: two ubiquitin-like systems. *Nat Rev Mol Cell Biol* **2**: 211–216
- Ren CM, Zhu Q, Gao BD, Ke SY, Yu WC, Xie DX, Peng W** (2008) Transcription factor WRKY70 displays important but no indispensable roles in jasmonate and salicylic acid signaling. *J Integr Plant Biol* **50**: 630–637
- Reuber TL, Ausubel FM** (1996) Isolation of *Arabidopsis* genes that differentiate between resistance responses mediated by the *RPS2* and *RPM1* disease resistance genes. *Plant Cell* **8**: 241–249
- Rojo E, Sharma VK, Kovaleva V, Raikhel NV, Fletcher JC** (2002) CLV3 is localized to the extracellular space, where it activates the *Arabidopsis* CLAVATA stem cell signaling pathway. *Plant Cell* **14**: 969–977
- Schmittgen TD, Livak KJ** (2008) Analyzing real-time PCR data by the comparative C(T) method. *Nat Protoc* **3**: 1101–1108
- Shah J** (2003) The salicylic acid loop in plant defense. *Curr Opin Plant Biol* **6**: 365–371
- Shah J** (2005) Lipids, lipases, and lipid-modifying enzymes in plant disease resistance. *Annu Rev Phytopathol* **43**: 229–260
- Shah J, Kachroo P, Klessig DF** (1999) The *Arabidopsis* *ssi1* mutation restores pathogenesis-related gene expression in *npr1* plants and renders defense gene expression salicylic acid dependent. *Plant Cell* **11**: 191–206
- Shah J, Tsui E, Klessig DF** (1997) Characterization of a salicylic acid-insensitive mutant (*sai1*) of *Arabidopsis thaliana*, identified in a selective screen utilizing the SA-inducible expression of the *tms2* gene. *Mol Plant Microbe Interact* **10**: 69–78
- Smith CJ** (1996) Accumulation of phytoalexins: defence mechanism and stimulus response system. *New Phytol* **132**: 1–45
- Smith DR, Kahng MW, Quintanilla-Vega B, Fowler BA** (1998) High-affinity renal lead-binding proteins in environmentally-exposed humans. *Chem Biol Interact* **115**: 39–52
- Thordal-Christensen H, Zhang Z, Wei Y, Collinge DB** (1997) Subcellular localization of H<sub>2</sub>O<sub>2</sub> in plants: H<sub>2</sub>O<sub>2</sub> accumulation in papillae and hypersensitive response during the barley-powdery mildew interaction. *Plant J* **11**: 1187–1194
- Xia Y, Suzuki H, Borevitz J, Blount J, Guo Z, Patel K, Dixon RA, Lamb C** (2004) An extracellular aspartic protease functions in *Arabidopsis* disease resistance signaling. *EMBO J* **23**: 980–988
- Xiao S, Chen QF, Chye ML** (2009) Light-regulated *Arabidopsis* ACBP4 and ACBP5 encode cytosolic acyl-CoA-binding proteins that bind phosphatidylcholine and oleoyl-CoA ester. *Plant Physiol Biochem* **47**: 926–933
- Xiao S, Chye ML** (2009) An *Arabidopsis* family of six acyl-CoA-binding proteins has three cytosolic members. *Plant Physiol Biochem* **47**: 479–484
- Xiao S, Chye ML** (2011) New roles for acyl-CoA-binding proteins (ACBPs) in plant development, stress responses and lipid metabolism. *Prog Lipid Res* **50**: 141–151



- Xiao S, Dai LY, Liu FQ, Wang ZL, Peng W, Xie DX (2004) COS1: an *Arabidopsis* coronatine insensitive1 suppressor essential for regulation of jasmonate-mediated plant defense and senescence. *Plant Cell* **16**: 1132–1142
- Xiao S, Gao W, Chen QF, Chan SW, Zheng SX, Ma J, Wang M, Welti R, Chye ML (2010) Overexpression of *Arabidopsis* acyl-CoA binding protein ACBP3 promotes starvation-induced and age-dependent leaf senescence. *Plant Cell* **22**: 1463–1482
- Xiao S, Gao W, Chen QF, Ramalingam S, Chye ML (2008a) Overexpression of membrane-associated acyl-CoA-binding protein ACBP1 enhances lead tolerance in *Arabidopsis*. *Plant J* **54**: 141–151
- Xiao S, Li HY, Zhang JP, Chan SW, Chye ML (2008b) *Arabidopsis* acyl-CoA-binding proteins ACBP4 and ACBP5 are subcellularly localized to the cytosol and ACBP4 depletion affects membrane lipid composition. *Plant Mol Biol* **68**: 571–583
- Yoshida S, Ito M, Nishida I, Watanabe A (2001) Isolation and RNA gel blot analysis of genes that could serve as potential molecular markers for leaf senescence in *Arabidopsis thaliana*. *Plant Cell Physiol* **42**: 170–178
- Yoshimoto K, Jikumaru Y, Kamiya Y, Kusano M, Consonni C, Panstruga R, Ohsumi Y, Shirasu K (2009) Autophagy negatively regulates cell death by controlling NPR1-dependent salicylic acid signaling during senescence and the innate immune response in *Arabidopsis*. *Plant Cell* **21**: 2914–2927
- Yurchenko OP, Nykiforuk CL, Moloney MM, Ståhl U, Banaś A, Stymne S, Weselake RJ (2009) A 10-kDa acyl-CoA-binding protein (ACBP) from *Brassica napus* enhances acyl exchange between acyl-CoA and phosphatidylcholine. *Plant Biotechnol J* **7**: 602–610
- Yurchenko OP, Weselake RJ (2011) Involvement of low molecular mass soluble acyl-CoA-binding protein in seed oil biosynthesis. *New Biotechnol* **28**: 97–109
- Zeng LR, Vega-Sánchez ME, Zhu T, Wang GL (2006) Ubiquitination-mediated protein degradation and modification: an emerging theme in plant-microbe interactions. *Cell Res* **16**: 413–426